Ab Initio Studies on the Mechanism of the Size-Dependent Hydrogen-Loss Reaction in $Mg^+(H_2O)_n$

Chi-Kit Siu and Zhi-Feng Liu*[a]

Abstract: The mechanism of size-dependent intracluster hydrogen loss in the cluster ions $Mg^+(H_2O)_n$, which is switched on around $n=6$, and off around $n=14$, was studied by ab initio calculations at the MP2/6-31G* and MP2/6-31G** levels for $n=1-6$. The reaction proceeds by Mg^+-assisted breaking of an H–O bond in one of the H_2O molecules. The reaction barrier is dependent on both the cluster size and the solvation structure. As n increases from 1 to 6, there is a dramatic drop in the reaction barrier, from greater than 70 kcal mol^{-1} for $n=1$ to less than 10 kcal mol^{-1} for $n=6$. In the transition structures, the Mg atom is close to the oxidation state of +2, and H_2O molecules in the first solvation shell are much more effective in stabilizing the transition structures and lowering the reaction barriers than H_2O molecules in the other solvation shells. While the reaction barrier for trimer core structures with only three H_2O molecules in the first shell is greater than 24 kcal mol^{-1}, even for $Mg^+(H_2O)_6$, it drops considerably for clusters with four–six H_2O molecules in the first shell. The more highly coordinated complexes have comparable or slightly higher energy than the trimer core structures, and the presence of such high coordination number complexes is the underlying kinetic factor for the switching on of the hydrogen-loss reaction around $n=6$. For clusters with trimer core structures, the hydrogen loss reaction is much easier when it is preceded by an isomerization step that increases the coordination number around Mg^+. Delocalization of the electron on the singly occupied molecular orbital (SOMO) away from the Mg^+ ion is observed for the hexamer core structure, while at the same time this isomer is the most reactive for the hydrogen-loss reaction, with an energy barrier of only 2.7 kcal mol^{-1} at the MP2/6-31G** level.

Keywords: ab initio calculations · cations · cluster compounds · hydrogen bonds

Introduction

The water-solvated Mg^+ ion forms an interesting system of ionic clusters that has been studied in great detail.[1–9] Recent experiments[9] showed that both $Mg^+(H_2O)_n$ and $(MgOH)^+(H_2O)_n$ are involved in hydrolysis and charge-transfer processes in $[Mg(H_2O)_n]^{2+}$, a subject of considerable interest to the study of the solvation around doubly charged metal cations.[10] The stability and reactivity of these clusters are also important, because they are intermediate between the gas and liquid phases.[10–14] As the size of the cluster ion grows, it approaches the liquid state and provides invaluable insights into solvation dynamics and reaction mechanisms in solution. In the case of Mg^+, a hydrogen-loss reaction [Eq. (1)] was observed when the cluster size n reached around 6.[1, 2] The reaction continued for increasing n up to around 14, when the reaction was turned off. This is a classical example of a size-dependent intracluster reaction, which has also been observed for ionic clusters with other types of solvent molecules or metal ions.[11–14]

$$Mg^+(H_2O)_n \rightarrow (MgOH)^+(H_2O)_{n-1} + H \quad (1)$$

The size-dependent hydrogen elimination reaction for $Mg^+(H_2O)_n$ is special in that there is a simple and convincing explanation for its switching on around $n=6$, based on thermodynamics.[1, 3] The $(MgOH)^+$ core of $(MgOH)^+(H_2O)_{n-1}$ is more polar than the Mg^+ core of $Mg^+(H_2O)_n$. As the cluster size grows, the additional water molecules stabilize the $(MgOH)^+$ core more than the Mg^+ core. Although $Mg^+(H_2O)_n$ is more stable than $(MgOH)^+(H_2O)_{n-1}$ for small n, as n increases, $(MgOH)^+(H_2O)_{n-1}$ becomes more stable starting at $n=6$, as verified by ab initio calculations.[3] The dominance of $(MgOH)^+(H_2O)_{n-1}$ signals in experiments for $n \geq 6$ is due to this shift of relative stability between $Mg^+(H_2O)_n$ and $(MgOH)^+(H_2O)_{n-1}$. The same explanation has been successfully extended to other ionic clusters, such as $Ca^+(H_2O)_n$,[15] $Mg^+(CH_3OH)_n$ and $Ca^+(CH_3OH)_n$.[16]

[a] Z.-F. Liu, C.-K. Siu
Department of Chemistry
The Chinese University of Hong Kong
Shatin, Hong Kong, China
Fax +852-2603-5057
E-mail: zfliu@cuhk.edu.hk

Supporting information for this article is available on the WWW under http://www.chemeurj.org or from the author.

  0947-6539/02/0814-3177 $ 20.00+.50/0

In contrast, the mechanism for the hydrogen loss reaction in $Mg^+(H_2O)_n$, and especially its dependence on size, have not attracted much attention. This may be partly due to the availability of a very successful explanation based on the energetics, and partly due to the fact that locating transition barriers for ionic clusters by ab initio calculations is nontrivial as the number of solvent molecules increases. Experimentally, the kinetic energy of an Mg^+ ion beam was adjusted before it interacted with water vapor to form cluster ions. It was found that increasing the kinetic energy of the Mg^+ beam only increased the signals of small clusters, but had no effect on the critical sizes for the hydrogen-loss reaction.[2] This observation was taken as proof that the reaction mechanism was not very important for the size-dependent effects.

However, a theoretical understanding of the mechanism of hydrogen loss is highly desirable before the mechanism factor can be safely ruled out. Although the critical sizes were not affected by the kinetic energy of Mg^+, this may simply indicate that the kinetic energy of Mg^+ is much more effective in promoting the evaporation of solvent molecules than promoting hydrogen elimination. Moreover, the mechanism, as well as its variation with increasing cluster size, should be a crucial part in our understanding of any size-dependent reaction. In the case of $B^+(H_2O)_n$ clusters,[17] an intracluster reaction to form $(HBOH)^+(H_2O)_{n-1}$ became spontaneous for $n \geq 3$. Our study on $Al^+(H_2O)_n$ clusters[18] revealed that a similar reaction proceeds to form $(HAlOH)^+(H_2O)_{n-1}$ for $n \geq 8$ within an elaborate network involving six water molecules in a ring structure and plays a significant role in size-dependent H_2 elimination. The reaction of $Al^+(H_2O)_n$ is especially interesting in comparison to the $Mg^+(H_2O)_n$ clusters, as it also exhibits on/off behavior that depends on cluster size, although the reactive range is between $n = 11$ and 24,[19, 20] as opposed to between $n = 6$ and 14 for $Mg^+(H_2O)_n$.[1, 2] With one less electron in the valence shell of Mg^+ than in that of Al^+, would there be a similar hydrogen transfer mechanism for $Mg^+(H_2O)_n$? The answer is interesting, since possible similarities between $Mg^+(H_2O)_n$ and $Al^+(H_2O)_n$ clusters were tentatively suggested before.[20] Finally, the switching on of hydrogen elimination occurs at a size of $n = 6$, which is lower than in many other systems, such as $Al^+(H_2O)_n$,[19] or $Na^+(CH_3OH)_n$.[21] A detailed search of the transition structures can be made by high-level ab initio calculations, and could potentially provide a model system for understanding size-dependent effects on reaction mechanisms. To the best of our knowledge, such a study has not been reported so far.

Methods of Calculation

Here we present the results of ab initio studies on $Mg^+(H_2O)_n$ ($n = 1-6$), with an emphasis on the transition structures and energy barriers involved in the hydrogen-loss reaction, and their variation with cluster size. All calculations were performed with the Gaussian 98 package.[22] Two basis sets are used in most calculations (6-31G* and 6-31G**). The structures of the singly charged $Mg^+(H_2O)_n$ clusters were first optimized by the unrestricted self-consistent field (UHF) method. Transition structures for the hydrogen-loss reaction were also first searched for at the UHF level. These stable and transition structures were then refined by further optimization at the second-order Møller–Plesset (MP2) level, and verified by the calculated vibrational frequencies. Natural population analyses[23] were evaluated at the MP2 level, and the population numbers are listed in the Supporting Information. For $Mg^+(H_2O)_n$ with $n = 1$ and 2, geometry optimizations were also performed at the QCISD level to verify the results.

Results and Discussion

$Mg^+(H_2O)$ and $Mg^+(H_2O)_2$: The stable structures of $Mg^+(H_2O)$ (**1+0**) in C_{2v} symmetry and $Mg^+(H_2O)_2$ (**2+0**) in C_2 symmetry are shown in Figures 1 and 2. The geometrical parameters are in good agreement with previous ab initio calculations.[1, 3, 24–27] Optimizations at the MP2 level brought little change to the structure parameters obtained at the UHF level, a fact that was noted before and attributed to the electrostatic nature of the Mg^+-H_2O interaction,[3, 25] which was little affected by electron correlation. Relative energy and transition barriers for $Mg^+(H_2O)$ and $Mg^+(H_2O)_2$ are tabulated in Table 1.

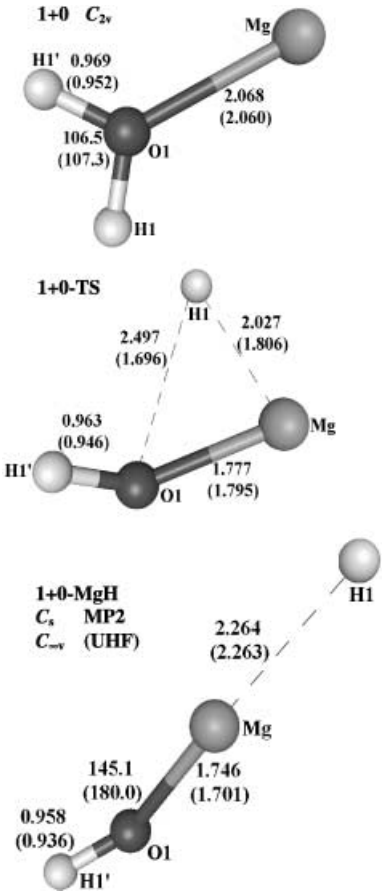

Figure 1. Optimized structures for $Mg^+(H_2O)$ and $H\cdots MgOH^+$ and the transition structure for Mg^+-assisted H–O bond breaking, with bond lengths [Å] and angles [°]. Values were obtained at the levels MP2/6-31G** and UHF/6-31G** (parentheses). In the designation of a structure, the first number indicates the number of water molecules in the first solvation shell, and the second number that in the second shell. This scheme is followed for all the figures.

Dissociation of $Mg^+(H_2O)_n$ clusters with loss of water molecules or a hydrogen atom on photo-induced electronic excitation was studied in detail by Fuke et al.[4, 5] and Duncan et al.[7, 8] The experimental observation was further expanded

  0947-6539/02/0814-3178 $ 20.00+.50/0 *Chem. Eur. J.* **2002**, *8*, No. 14

Table 1. Relative energies and transition barriers for $Mg^+(H_2O)$ and $Mg^+(H_2O)_2$.

	Relative energy [kcal mol^{-1}]						Energy barrier [kcal mol^{-1}]					
	UHF		MP2		QCISD		UHF		MP2		QCISD	
	6-31G*	6-31G**	6-31G*	6-31G**	6-31G*	6-31G**	6-31G*	6-31G**	6-31G*	6-31G**	6-31G*	6-31G**
1 + 0	0.0	0.0	0.0	0.0	0.0	0.0	77.5	79.8	68.5	71.9	67.6	72.1
1 + 0-MgH	69.6	72.5	63.7	69.0	65.8	71.2						
2 + 0	0.0	0.0	0.0	0.0	0.0	0.0	54.1	56.1	45.5	49.0	44.7	49.1
2 + 0-MgH	45.8	48.7	41.3	46.9	43.6	49.2						

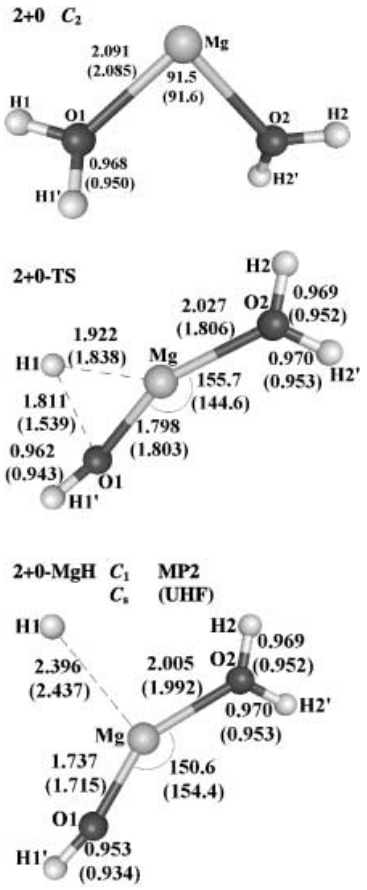

Figure 2. Optimized structures for $Mg^+(H_2O)_2$ and $H\cdots MgOH^+(H_2O)$ and the transition structure for Mg^+-assisted H–O bond breaking, with bond lengths [Å] and angles [°]. Values were obtained at the levels MP2/6-31G** and UHF/6-31G** (parentheses). For the designation of the structures, see legend to Figure 1.

by calculations on the electronic structures and energetics for small $Mg^+(H_2O)_n$ clusters.[4, 6, 26] However, to the best of our knowledge, there have been no reports on the mechanism of Mg^+ insertion into an O–H bond of H_2O. Sakai[28] studied such an insertion process for the neutral Mg atom, both in the ground state ^1S and the excited state ^3P, with structures optimized at the UHF/6-31G(d,p) level and energies calculated at the MP2 and MP4 levels. For the ^1S state, it led to a stable product H–Mg – OH. For the ^3P excited state, the electronic excitation weakened the H–Mg bond, the interaction between Mg and H became repulsive, and H was lost.

For the ionic Mg^+ ground state ^2S, insertion into an H–O bond produces $H\cdots Mg^+$–OH with very weak $H\cdots Mg$ interaction. As shown in Figure 1, the $H\cdots Mg$ distance is 2.264 Å at the MP2/6-31G** level, compared to a value of 1.706 Å in the neutral and stable ground state HMgOH.[28] According to natural population numbers, the H atom in $H\cdots Mg^+$–OH is almost neutral and bears the unpaired electron. It contributes little to stabilization of the ion, as Mg is oxidized from the +1 to the +2 state. The charge distribution in the transition structure leading to Mg^+ insertion is similar to that in $H\cdots Mg^+$–OH. The H atom forms a triangle with O and Mg^+ in the transition structure and has a slightly positive charge. At the UHF/6-31G** level, the O1–H1 distance is 1.696 Å. However, at the MP2 level, the distance is increased significantly to 2.497 Å. For further verification, we optimized the transition state **1 + 0-TS** with a large basis set (6-311 + + G**) and at better correlation levels (MP4, and QCISD(T)), each starting with the UHF/6-31G** transition structure. The O1–H1 distance was again found to be more than 2.2 Å. Such a large distance indicates that the O1–H1 bond is already broken in **1 + 0-TS**, and the assistance of Mg^+ to O–H bond breaking is very small.

Thus, the $H\cdots Mg^+$–OH ion is in sharp contrast to the H–Al^+ – OH ion, which was studied by Schwarz et al.[29] The H–Al distance in H–Al^+–OH was only around 1.54 Å, and homolysis of the H–Al bond would require more than 70 kcal mol^{-1}. The difference is most likely due to the fact that H–Al^+–OH is an ion with a closed shell, while there is an unpaired electron in $H\cdots Mg^+$–OH. As a result, the hydrogen-loss reaction in $Mg^+(H_2O)_n$ should be completely different from the H_2 loss reaction in $Al^+(H_2O)_n$.

Our recent study found that $Al^+(H_2O)_n$ isomerized spontaneously into $HAlOH^+(H_2O)_{n-1}$ for $n \geq 8$. $HAlOH^+(H_2O)_{n-1}$ was also more stable than $Al^+(H_2O)_n$ for $n \geq 2$,[17] and the isomerization barrier dropped significantly as the cluster size increased.[18] In contrast, structure optimizations starting with H–$MgOH^+(H_2O)_{n-1}$ always led to a long $H\cdots Mg$ distance ($\geq$2.2 Å).

Relative to $Mg^+(H_2O)$, the calculated energy with zero-point corrections is 63.7 kcal mol^{-1} for $H\cdots(MgOH)^+$ at the MP2/6-31G* level (Table 1), which is slightly more stable than the relative energy of 66.8 kcal mol^{-1} for the dissociated $(MgOH)^+ + H$, also at the MP2/6-31G* level, as previously reported.[3] This is another indication that the H atom in $H\cdots(MgOH)^+$ is almost free to leave. The reaction barrier for the insertion is 71.9 kcal mol^{-1} at the MP2/6-31G** level, accessible only by electronic excitation.

The optimized structures for $Mg^+(H_2O)_2$ are shown in Figure 2. As n increases from 1 to 2, there is a substantial decrease both in the overall energetics and the reaction barrier for the transformation from $Mg^+(H_2O)_2$ to $H\cdots(MgOH)^+(H_2O)$. At the MP2/6-31G** level, the reaction energy is now 46.9 kcal mol^{-1} and the barrier 49.0 kcal mol^{-1}

  0947-6539/02/0814-3179 $ 20.00+.50/0

(Table 1). The O1-H1 distance in **2 + 0-TS** is now 1.811 Å. Compared to the value of 2.497 Å for $Mg^+(H_2O)$, it indicates a larger role for Mg^+ in the O–H bond-breaking process. This trend continues for larger n (see below).

Although electronic correlation effects are not important for the ground-state energy and geometry of the $Mg^+(H_2O)_n$ cluster ions,[3, 25] the transition structures and energy barriers are changed significantly when correlation effects are included, as shown in Figure 1 and Table 1. For $n = 1$ and 2, additional calculations were performed at the QCISD/6-31G** level, and the good agreement with the MP2 results (Table 1) indicates that the correlation effect for these cluster ions and their transition structures could be adequately addressed at the MP2 level.

Structures of $Mg^+(H_2O)_n$ ($n = 3-6$): For $Mg^+(H_2O)_n$ ($n = 3-6$), the stable structures are shown in Figures 3, 4, 5, and 6, and transition structures in Figures 3, 4, 7, and 8; relative energies and reaction barriers are listed in Table 2; for natural population numbers, see Supporting Information. With increasing number of water molecules in $Mg^+(H_2O)_n$, there are alternative ways to arrange these molecules in various solvation shells. One way is to place all water molecules in the first shell, as studied at the MP2/6-31G** level by Castleman et al.[1] However, it is generally understood that hydrogen bonding between water molecules could be comparable in strength to the direct bonding between Mg^+ and H_2O, since the unpaired electron on Mg^+ interacts repulsively with water molecules when the first shell becomes too

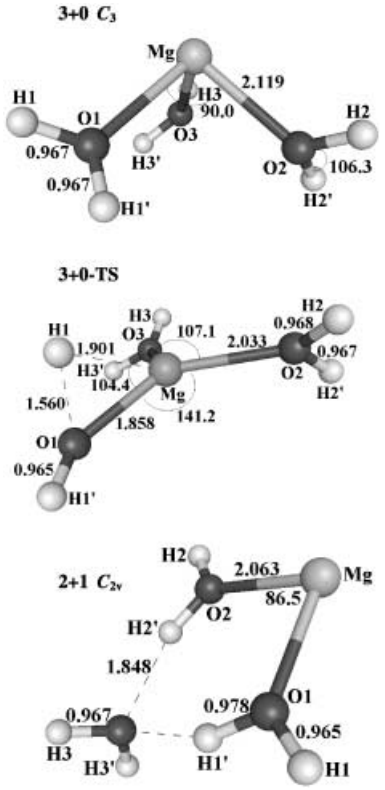

Figure 3. Optimized structures for $Mg^+(H_2O)_3$, with bond lengths [Å] and angles [°]. **3 + 0** is a trimer core structure, and **2 + 1** a dimer core structure. Optimized transition structures for Mg^+-assisted H–O bond breaking are named after the corresponding reactants. All values were obtained at the MP2/6-31G** level. For the designation of the structures, see legend to Figure 1.

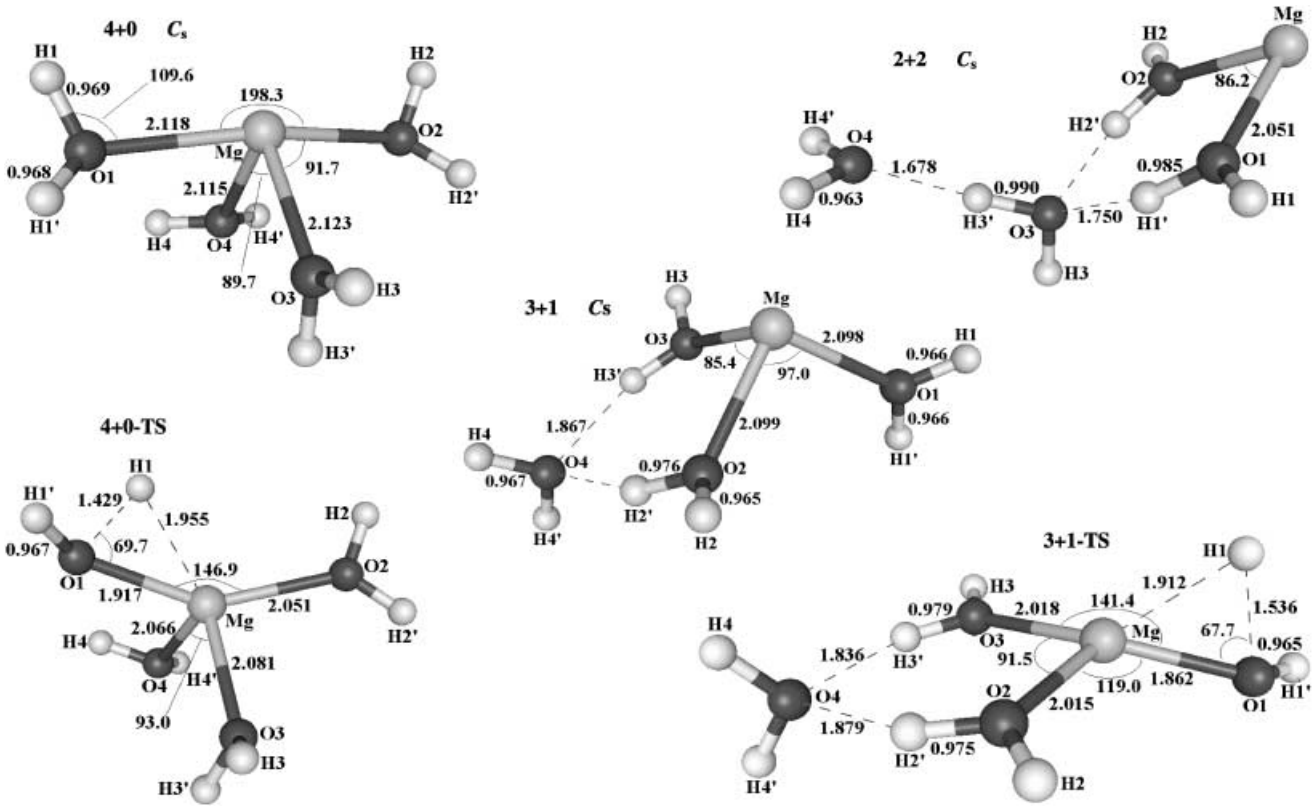

Figure 4. Optimized structures for $Mg^+(H_2O)_4$. **4 + 0** is a tetramer core structure, **3 + 1** a trimer core structure, and **2 + 2** a dimer core structure. Optimized transition structures for Mg^+-assisted H–O bond breaking are named after their corresponding reactants. Bond lengths [Å] and angles [°] are shown. All values were obtained at the MP2/6-31G** level. For the designation of the structures, see legend to Figure 1.

  0947-6539/02/0814-3180 $ 20.00+.50/0 *Chem. Eur. J.* **2002**, *8*, No. 14

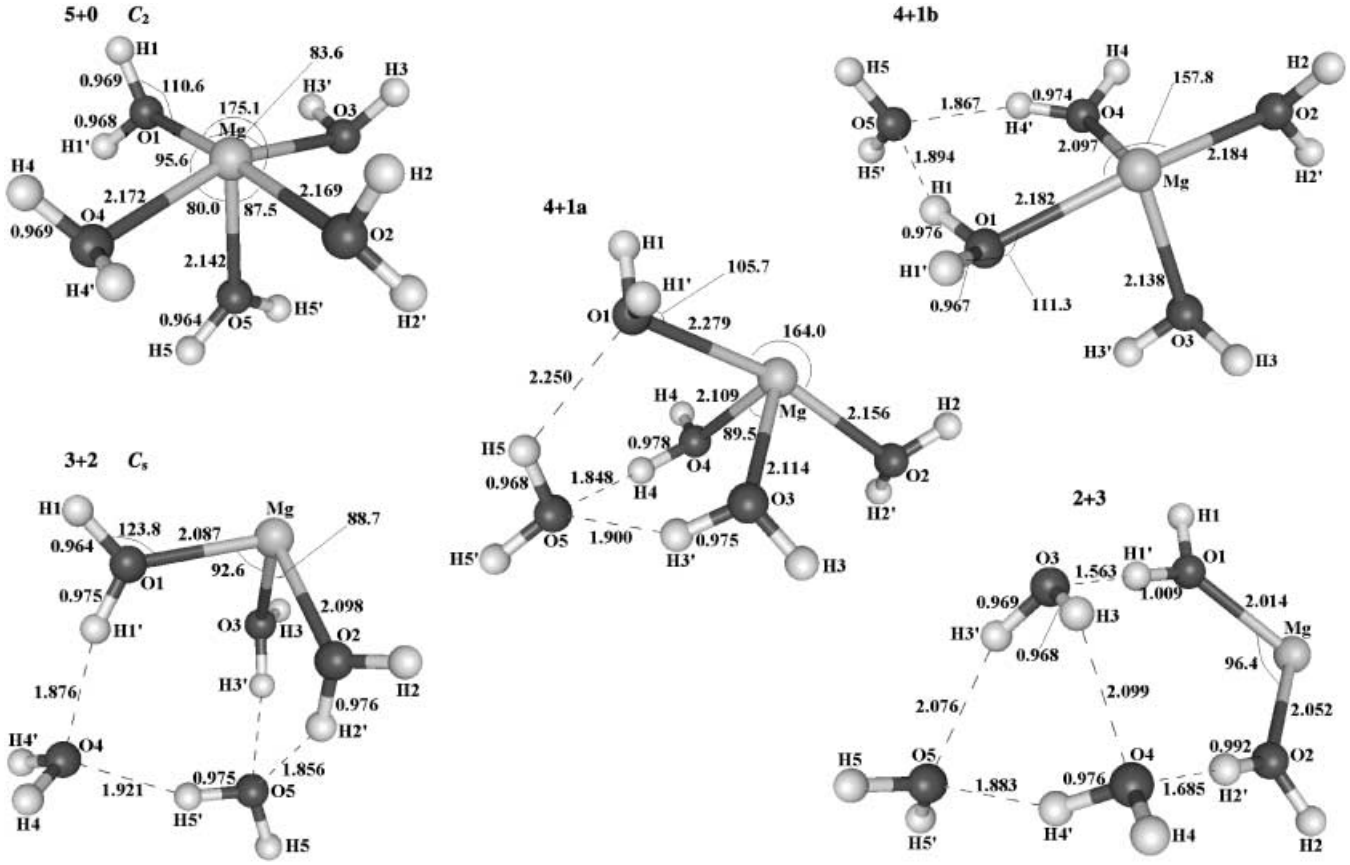

Figure 5. Optimized structures for $Mg^+(H_2O)_5$. **5 + 0** is a pentamer core structure, **4 + 1a** and **4 + 1b** tetramer core structures, **3 + 2** a trimer core structure, and **2 + 3** a dimer core structure. The bond lengths [Å] and angles [°] were all obtained at the MP2/6-31G** level. For the designation of the structures, see legend to Figure 1.

Table 2. Relative energy and transition barriers for $Mg^+(H_2O)_n$ ($n = 3-6$). For each size n, the energy of a trimer core structure is used as the reference.

	Relative energy [kcal mol^{-1}]				Energy barrier [kcal mol^{-1}]			
	UHF		MP2		UHF		MP2	
	6-31G*	6-31G**	6-31G*	6-31G**	6-31G*	6-31G**	6-31G*	6-31G**
3 + 0	0.0	0.0	0.0	0.0	39.4	41.3	31.1	33.9
2 + 1	4.7	4.8	4.5	4.3				
4 + 0	2.2	2.2	1.0	1.2	25.8	27.4	18.3	20.8
3 + 1	0.0	0.0	0.0	0.0	37.2	39.1	28.5	31.5
2 + 2	7.9	8.0	8.1	7.8				
5 + 0	4.2	4.4	1.2[b]	1.5	17.3	18.8	10.4	12.5
4 + 1a	2.5	2.6	0.9	1.1	23.1	24.8	13.8	16.2
4 + 1b	0.7	0.8	− 0.3	− 0.2	25.3	26.8	15.8	17.9
3 + 2	0.0	0.0	0.0[b]	0.0	39.9[a]	41.7 [a]	31.4[a]	32.6
2 + 3	9.9	9.9	11.5	10.9				
6 + 0	14.5	14.8	2.7	3.8	3.7	5.0	1.7	2.7
5 + 1	2.4	2.7	− 2.1	− 1.6	15.4	16.9	7.1	9.0
4 + 2a	0.1	0.1	− 2.0	− 1.8				
4 + 2b	1.3	1.4	− 0.5	− 0.4	20.2	21.7	10.1	12.4
4 + 2c	1.2	1.1	− 0.1	0.1	20.8	22.7	10.0	12.3
3 + 3	0.0	0.0	0.0	0.0	34.3	36.4	22.0	24.9

[a] Two imaginary frequencies. [b] One imaginary frequency.

crowded.[24] In the case of $Al^+(H_2O)_n$,[17] for which the repulsive interaction is more prominent due to the lone pair on Al^+, the maximum number of water molecules in the first shell was found to be three, which was termed the "trimer core structure",[17] while water molecules in the second and third solvation shells would form hydrogen-bonded networks together with the first-shell ligands. Tetramer core structures were unstable.[17, 18, 24]

Trimer core structures were also found to be the most stable structures for $Mg^+(H_2O)_n$, and studied in great detail by Iwata et al. for $n = 3-6$.[3] However, in the case of $n = 4$, the most stable trimer core structure is only slightly lower in energy than the tetramer core structure (**3 + 1** and **4 + 0** in Figure 4). The energy gap is around 6 kcal mol^{-1} at the SCF/6-31G level,[3] but decreases further to 4 kcal mol^{-1} when a larger basis set is used (SCF/6-31G* optimized geometry and SCF/TZ2P evaluated energy).[24] When correlation is taken into account at the MP2 level in our calculation (Table 2), the energy difference falls within the expected accuracy of these calculations, and indicates that structures with higher coordination numbers in the first shell may be much more important for $Mg^+(H_2O)_n$ than for $Al^+(H_2O)_n$.

We hence further investigated the relative stability of these structures for $n = 5$ (Figure 5) and 6 (Figure 6), for which pentamer and hexamer cores are also possible. As shown in Table 2, the energy difference between trimer and tetramer core structures could switch from positive to negative values depending on the level of theory, while its absolute value at the MP2/6-31G** level is within 2 kcal mol^{-1} and within the expected accuracy of our calculation. Each type of structure could have further small variations in the hydrogen-bonded

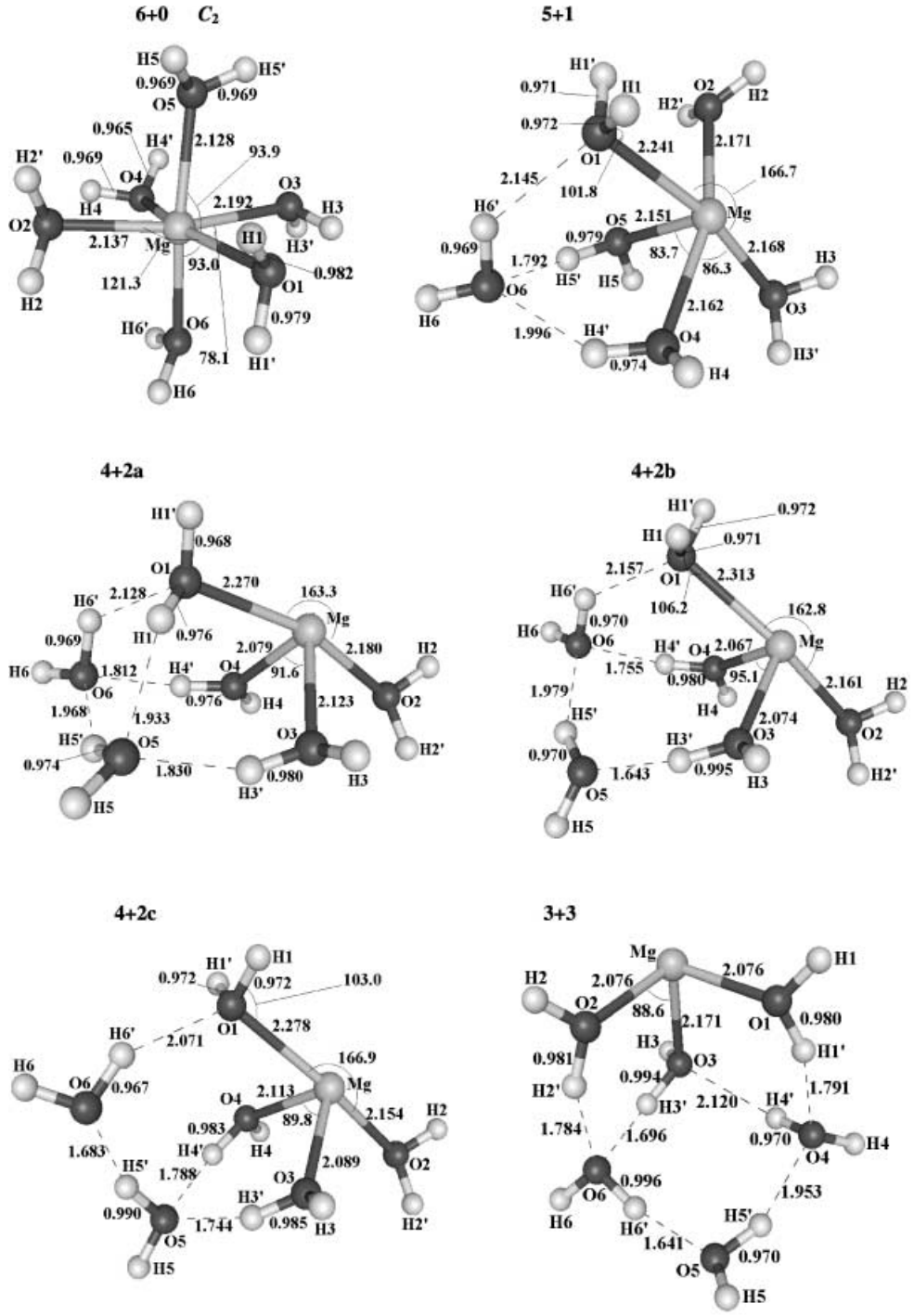

Figure 6. Optimized structures for $Mg^+(H_2O)_6$. **6+0** is a hexamer core structure, **5+1** a pentamer core structure, **4+2a**, **4+2b**, and **4+2c** tetramer structures, and **3+3** a trimer core structure. The bond lengths [Å] and angles [°] were all optimized at the MP2/6-31G** level. For the designation of the structures, see legend to Figure 1.

network, which produce a number of isomers (e.g., **4+1a** and **4+1b** in Figure 5; **4+2a**, **4+2b**, and **4+2c** in Figure 6), that lie close to each other in energy.

At the UHF level, pentamer core and hexamer core structures are clearly higher in energy than their trimer and tetramer core isomers. However, the inclusion of correlation effects by the MP2 method reduces the energy difference to around 5 kcal mol^{-1}. As the number of first-shell water molecules increases from 3 to 5, the positive charge on Mg^+ decreases, according to natural population analysis, which indicates greater charge donation from O to Mg^+ by covalent bonding. Correlation effects thus become more important as the coordination number around Mg^+ increases. Previous studies on neutral $Na(H_2O)_n$ clusters, which are isoelectronic with $Mg^+(H_2O)_n$, investigated the energy difference between "surface" and "interior" complexes,[30, 31] where the surface complex roughly correspond to smaller core clusters, and the interior complex to larger core clusters. At the correlated level of theory with large basis sets, the total energies for these structures are very close to each other.[32] Similarly, complexes

  0947-6539/02/0814-3182 $ 20.00+.50/0 *Chem. Eur. J.* **2002**, *8*, No. 14

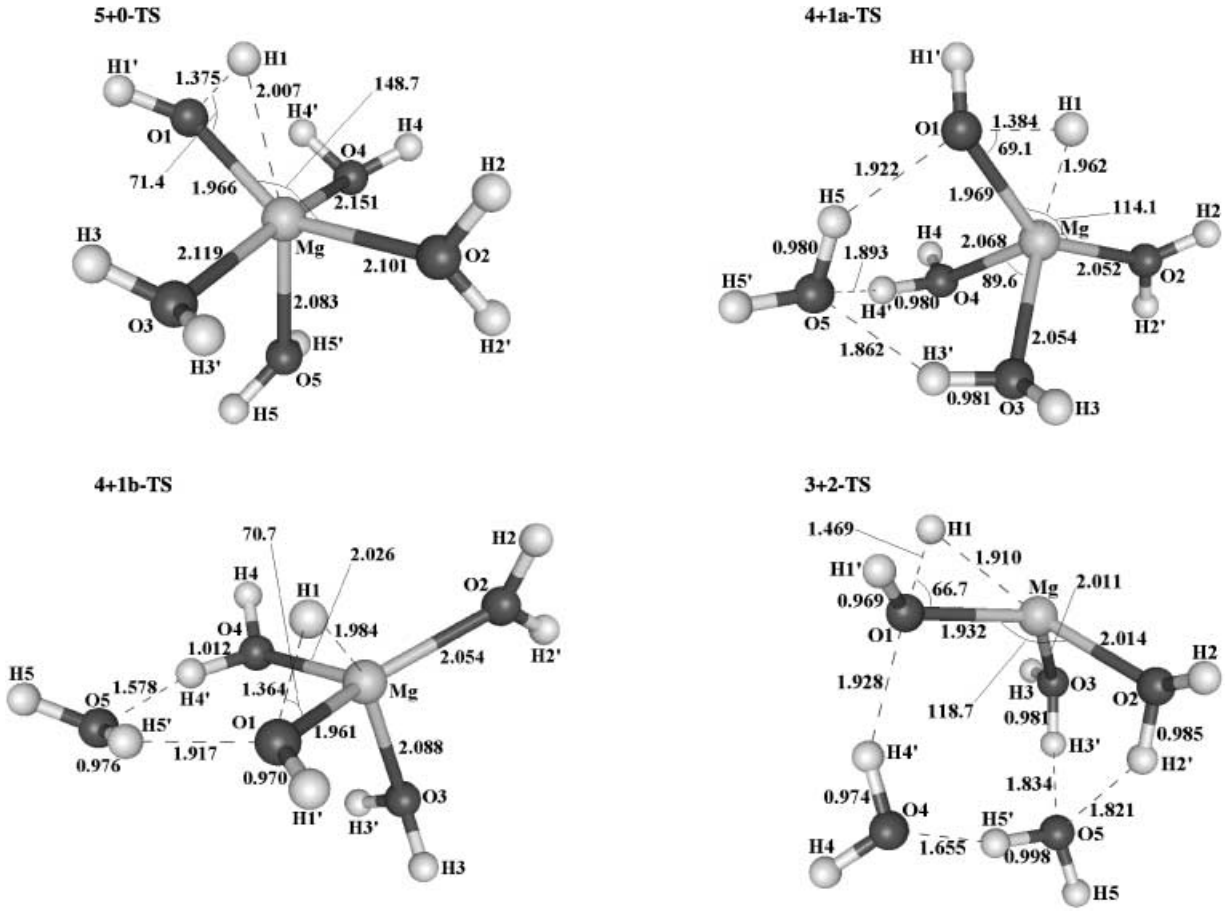

Figure 7. Transition structures for Mg^+-assisted H–O bond breaking in $Mg^+(H_2O)_5$, named after their corresponding reactants in Figure 5. The bond lengths [Å] and angles [°] were all optimized at the MP2/6-31G** level.

with high coordination numbers in the first shell (up to 5) were also found for $Li(H_2O)_n$.[33] In this respect, the $Mg^+(H_2O)_n$ cluster ions are similar to $Na(H_2O)_n$ and $Li(H_2O)_n$, rather than $Al^+(H_2O)_n$. The repulsive effect of an unpaired electron on Na or Mg^+ is much less than that of the electron lone pair on Al^+.

We also considered several other factors that could effect the relative energies among these isomers with varying core sizes. The thermal and entropic factors are included in the relative enthalpy and free energy, as listed in Table 3, and the correction has little effect on the relative stability. However, the basis set superposition error (BSSE), as estimated at the MP2/6-31G** level by the counterpoise correction method, and also listed in Table 3, is more significant. The magnitude of correction is larger for isomers with a larger core, and this can be attributed to the more compact geometric configurations for these isomers. Interestingly, with BSSE correction included, there is an identifiable trend of relative stability for $Mg^+(H_2O)_n$ ($n = 5, 6$), for which the trimer core structure is most stable and the energy increases with increasing core size. The energy difference is within 4 kcal mol^{-1}, except for the hexamer core structure of $Mg^+(H_2O)_6$, for which the energy relative to the trimer core isomer is a more substantial 11.9 kcal mol^{-1}.

These results lead us to the conclusion that experimentally studied $Mg^+(H_2O)_n$ cluster ions are a mixture in which the number of water molecules in the first solvation shell varies from three to five, as was also suggested in a recent theoretical study on the photodissociation excitation spectra of $Mg^+(H_2O)_n$.[6] These complexes with high coordination number (>3) turn out to be very important in the mechanism of the hydrogen-loss reaction.

Table 3. Relative energies, corrected for BSSE, thermal, and entropic factors at the MP2/6-31G** level. For each size n, the energy of a trimer core structure is used as the reference.

	ΔE [kcal mol^{-1}]	ΔE_{BSSE} [kcal mol^{-1}]	$\Delta H_{298\,K}$ [kcal mol^{-1}]	$\Delta S_{298\,K}$ [cal mol^{-1} K^{-1}]	$\Delta G_{298\,K}$ [kcal mol^{-1}]
3+0	0.0	0.0	0.0	0.0	0.0
2+1	4.3	2.2	3.8	−3.0	4.7
4+0	1.2	3.4	1.5	1.1	1.2
3+1	0.0	0.0	0.0	0.0	0.0
2+2	7.8	4.6	7.6	0.8	7.3
5+0	1.5	6.4	2.2	2.2	1.5
4+1a	1.1	4.5	0.9	−3.5	2.0
4+1b	−0.2	1.8	0.0	0.5	−0.2
3+2	0.0	0.0	0.0	0.0	0.0
2+3	10.9	9.6	10.7	0.2	10.7
6+0	3.8	11.9	4.9	3.7	3.8
5+1	−1.6	3.4	−1.1	0.3	−1.2
4+2a	−1.8	0.7	−1.5	0.1	−1.5
4+2b	−0.4	0.8	0.4	6.4	−1.5
4+2c	0.1	1.8	0.6	3.6	−0.5
3+3	0.0	0.0	0.0	0.0	0.0

Mechanism of hydrogen loss for $Mg^+(H_2O)_n$ ($n=3-6$): For $Mg^+(H_2O)_n$ ($n=3-6$) we again studied the hydrogen-loss reaction involving Mg^+-assisted O–H bond breaking, similar to that for $Mg^+(H_2O)$ and $Mg^+(H_2O)_2$.

Transition structures are shown in Figure 3 for $n=3$, Figure 4 for $n=4$, Figure 7 for $n=5$, and Figure 8 for $n=6$. The reaction barriers are listed in Table 2. Although the barrier for hydrogen loss is fairly high for $Mg^+(H_2O)_n$, ($n=1$, 2), it gradually decreases as the size of the cluster ion increases, from more than 30 kcal mol^{-1} for $n=3$, to about 20 kcal mol^{-1} for $n=4$, about 10 kcal mol^{-1} for $n=5$, and less than 10 kcal mol^{-1} for $n=6$. Thus, the barrier is size-dependent and should be a contributing factor in the observed switching on of the hydrogen-loss reaction around $n=6$. The length of the broken O–H bond is decreased to around 1.5 Å or less for all transition structures, and there seems to be a correlation between a lower value of this distance and a lower value of the reaction barrier.

The decrease in reaction barriers could be explained by the same reason underlying the switch in the relative stability between $Mg^+(H_2O)_n$ and $(MgOH)^+(H_2O)_{n-1}$ with increasing n.[3] According to the natural population analysis, the charge on the departing hydrogen atom is slightly negative (around -0.1) in the transition structures, while the charge on Mg of around $+1.7$ indicates that the Mg atom is fairly close to its final $+2$ oxidation state and becomes more polar during the reaction. As the number of water molecules increases, the Mg^{2+} ion becomes increasingly stabilized, and as a result, there is a dramatic decrease in the reaction barrier for hydrogen loss.

For the same reason, the barrier height is also affected by the solvation structure. For each cluster size n ($n=3-6$), we located several transition structures with varying coordination number around Mg. For $Mg^+(H_2O)_n$ with a trimer core, the reaction barrier changes only slightly and stays fairly high at around 30 kcal mol^{-1} as n increases from 3 to 5. A more noticeable drop occurs at $n=6$, but the value is still 24.9 kcal mol^{-1} at the MP2/6-31G** level. In contrast, for a fixed cluster size, the reaction barrier drops by more than 10 kcal mol^{-1} on going from the trimer core to the tetramer, and the decrease is more prominent for larger n (e.g., $n=6$, Table 2). In addition, the barrier decreases further on going from tetramer to pentamer and then hexamer structures. These trends are due to the fact that the water molecules in the first shell interact directly with the Mg^{2+} ion and are thus much more effective in stabilizing the oxidized Mg^{2+} ion than water molecules in the second or higher solvation shells. It also explains the fact that we were unable to locate hydrogen-loss transition structures for any of the dimer core isomers of $Mg^+(H_2O)_n$ with $n \geq 3$.

Due to their stability relative to other isomers, trimer core structures will be a significant component in the experimental beam of $Mg^+(H_2O)_n$. To maintain only three H_2O molecules in the first solvation shell, additional water molecules would have to enter the second or higher solvation shells and remain remote from direct interaction with the Mg ion, even when a trimer core cluster grows in size. These water molecules will not be very effective in stabilizing the polar Mg^{2+} ion. The hydrogen loss reaction barrier found for **3 + 3-TS** of 24.9 kcal mol^{-1} could thus be taken as an approximate lower limit for $Mg^+(H_2O)_n$ clusters of any size with trimer core structures. As a result, the reaction rate for trimer core $Mg^+(H_2O)_n$ clusters will be low. In contrast, the tetramer, pentamer, and hexamer core structures are much more favorable for the hydrogen-loss reaction, as shown in Table 2, and the presence of these isomers is the kinetic factor underlying the experimentally observed switching on of the hydrogen-loss reaction around $n=6$.[1, 2] The same kinetic factor should also be important for the observation of hydrogen-loss reactions in $Ca^+(H_2O)_n$[2, 15] and $Mg^+(CH_3OH)_n$ clusters.[16]

It is also conceivable that clusters with a trimer core first go through an isomerization process to increase the number of water molecules in the first shell, and then the hydrogen-loss reaction takes place. Since the potential surfaces for $Mg^+(H_2O)_n$ exhibit many minima, the isomerization barriers are expected to be low, and the number of isomerization paths should increase with growing cluster size. For $Mg^+(H_2O)_5$ and $Mg^+(H_2O)_6$, we identified several barriers, as listed in Table 4.

Table 4. Isomerization energies for increasing the core size by one water molecule. Values in parentheses include BSSE correction.

	Relative energy [kcal mol^{-1}]		Energy barrier [kcal mol^{-1}]	
	UHF/6-31G**	MP2/6-31G**	UHF/6-31G**	MP2/6-31G**
4 + 1b	0.8	−0.2 (1.8)	5.8	4.7 (6.2)
3 + 2	0.0	0.0 (0.0)	5.0	5.3 (6.2)
4 + 2c	1.1	0.1 (1.8)	4.1	3.2 (5.1)
3 + 3	0.0	0.0 (0.0)	4.4	2.5 (3.4)

Their values, which range from 3 to 6 kcal mol^{-1}, are significantly lower than the hydrogen-loss barriers listed in Table 2.

Hexamer core structure of $Mg^+(H_2O)_6$ and switching off of the hydrogen-loss reaction for larger clusters: Although the hexamer core structure of $Mg^+(H_2O)_6$ (**6 + 0**) is noticeably less stable than the other isomers, it nonetheless deserves special attention because its charge distribution is qualitatively different from those of the others. For $Mg^+(H_2O)_6$, the positive charge on the Mg^+ ion decreases from 0.95 for the trimer core structure **3 + 3** to 0.94 for the tetramer core structures **4 + 2a**, **4 + 2b**, **4 + 2c**, and to 0.92 for the pentamer core **5 + 1**. A similar trend is observed for $Mg^+(H_2O)_4$ and $Mg^+(H_2O)_5$. It indicates more charge donation from the oxygen atoms to Mg^+ as more water ligands are included in the first solvation shell, while the singly occupied orbital is basically localized on Mg^+.

However, the charge on Mg for the hexamer core structure **6 + 0** suddenly jumps to $+1.16$ at the MP2/6-31G** level, which indicates a reversal in charge transfer, whereby negative charge goes from Mg^+ to the surrounding H_2O ligands. The situation is quite similar to the neutral $Na(NH_3)_n$ clusters studied in detail by Hashimoto and Morokuma.[34] Charge transfer from NH_3 to Na was observed up to $n=4$, but for $n \geq 5$, the transfer was reversed and went from Na to NH_3.

  0947-6539/02/0814-3184 $ 20.00+.50/0 *Chem. Eur. J.* **2002**, *8*, No. 14

The SOMO became diffusive and was distributed among the Na and N atoms. As a result, inclusion of diffusive basis functions increased the flow of charge from the Na atom. For **6 + 0**, we performed further calculations with additional diffusive basis functions in the basis sets 6-31++G** and 6-311++G**, and the positive charge on the Mg atom indeed increased further to greater than 1.4.

Sodium/ammonia solution is a well-known system in which the sodium atoms are ionized and the valence electrons are solvated by ammonia molecules.[35, 36] The existence of such solvated ion pairs has also been suggested and explored for the clusters $M(H_2O)_n$ (M = Li, Na) in the form of $M^+(H_2O)_m(H_2O)_l(H_2O)_{n-m-l}^-$.[37] The diffusive SOMO in **6 + 0**, in analogy to $Na(NH_3)_n$, seems to indicate the existence of such ion pairs for large $Mg^+(H_2O)_n$ clusters as well. In fact such ion pairs have been invoked before as a possible reason for the switching off of the hydrogen-loss reaction in $Mg^+(H_2O)_n$ for $n > 14$.[2]

However, this explanation is problematic from a mechanistic point of view. Although **6 + 0** is a local minimum with all-real vibrational frequencies, it nonetheless has a very low barrier for the hydrogen-loss reaction (2.7 kcal mol^{-1} at the MP2/6-31G** level). The mechanism is also somewhat different from the other types of core structures in which the Mg^+ ion assists in H–O bond breaking. For **6 + 0**, hydrogen is lost by a simple stretching of the H–O bond, and the H atom is shielded from the Mg atom, as in **6 + 0-TS** (Figure 8). From an energetic perspective, hexamer core structures may well exist for the larger $Mg^+(H_2O)_n$ clusters, but judging from the reaction barrier, they would facilitate hydrogen loss, rather than turning the reaction off.

The switching-off mechanism should be influenced by both the possible presence of solvated-electron ion pairs and the barrier height for the hydrogen loss reaction in these ion pairs. Both factors are probably also size-dependent. A clarification of their interplay would have to wait for more detailed simulations on the $Mg^+(H_2O)_n$ clusters of larger sizes ($n > 6$).

Conclusion

In summary, we have studied the mechanism for the intracluster hydrogen-loss reaction in $Mg^+(H_2O)_n$ involving Mg^+-assisted H–O bond breaking in one of the H_2O molecules. Based on the transition structures located by ab initio calculations, the reaction barrier is size-dependent and decreases significantly from above 70 kcal mol^{-1} to around 10 kcal mol^{-1} or less as n increases from 1 to 6.

Among the isomers of the $Mg^+(H_2O)_n$ clusters, structures with high coordination numbers (> 3) in the first solvation shell around Mg^+ are comparable or only slightly higher in energy than the trimer core structures, especially when correlation effects are included in the ab initio calculations. This conclusion remains valid after BSSE and thermal and

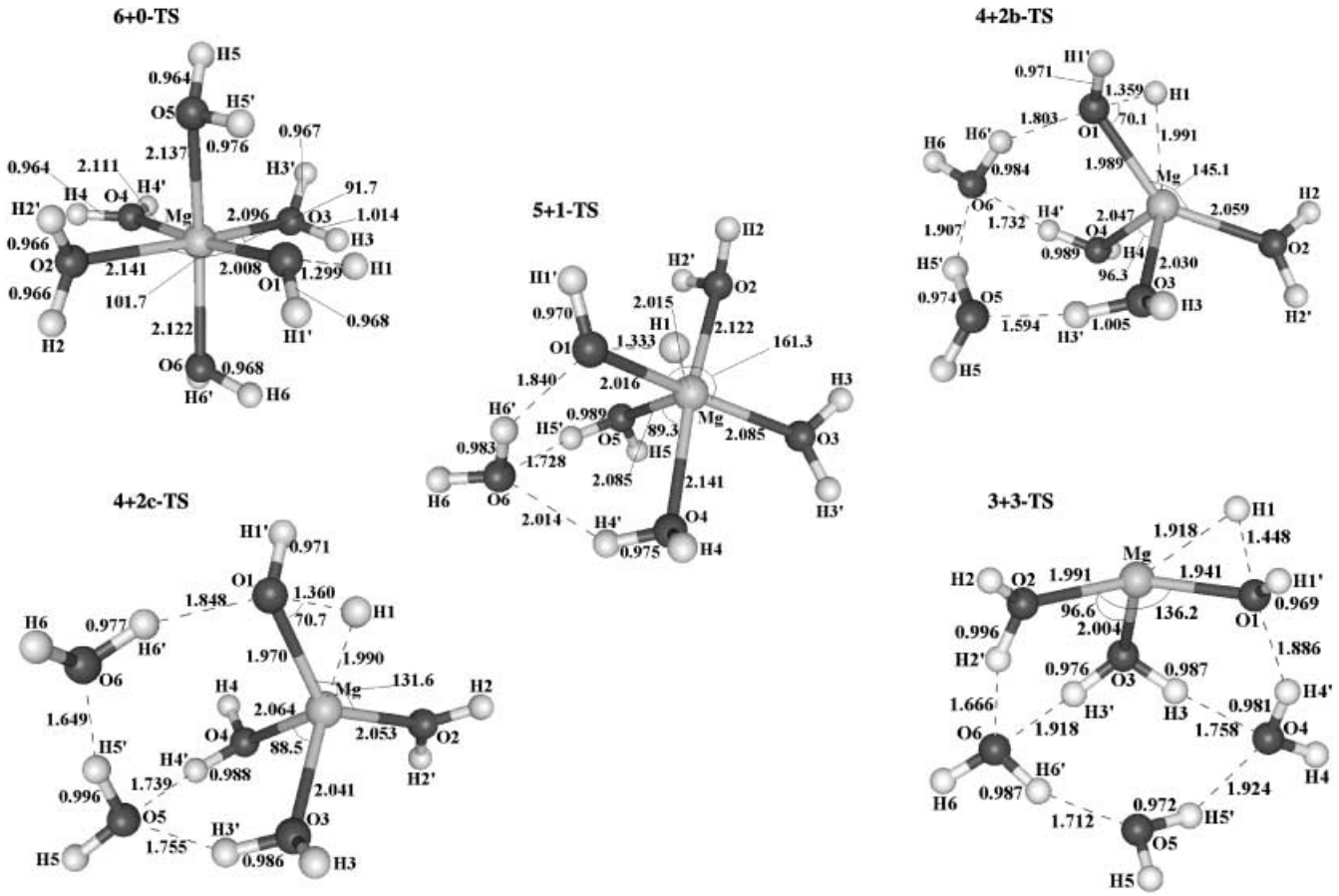

Figure 8. Transition structures for Mg^+-assisted H–O bond breaking in $Mg^+(H_2O)_6$, named after their corresponding reactants in Figure 7. The bond lengths [Å] and angles [°] were all optimized at the MP2/6-31G** level.

entropic factors are taken into consideration. As water molecules in direct interaction with the Mg ion are more effective in stabilizing the oxidized Mg ion during the hydrogen-loss reaction, the reaction barrier for tetramer, pentamer, and hexamer core structures is significantly lower than that for the trimer core structure. Kinetically, the experimentally observed switch-on of the hydrogen-loss reaction around $n=6$ is due to the presence of such clusters with high coordination numbers (>3). For the trimer core structures, it is more favorable for the hydrogen-loss reaction to go through two steps, first an isomerization step to increase the coordination number of Mg^+, and then Mg^+-assisted H–O bond breaking.

The hexamer core structure **6 + 0** is unique among the $Mg^+(H_2O)_6$ isomers studied in that its SOMO is diffusive, and charge flows from Mg^+ to the surrounding water molecules. On the other hand, the barrier of hydrogen loss for **6 + 0** is very low ($2.7\,kcal\,mol^{-1}$), and H–O bonds could break without assistance from Mg^+. Whether the presence of such structures contributes to the switching off of the hydrogen-loss reaction for $n>14$, as suggested in previous studies, remains unresolved, and an answer has to wait for more detailed simulations on larger clusters.

Acknowledgements

Calculations reported in this paper were performed on the AlphaStation clusters operated by the Department of Chemistry, the Chinese University of Hong Kong (CUHK), supported by a Special Equipment Grant, and on the SGI Origin 2000, at the Information Technology Services Center (ITSC), CUHK. We thank Mr. Ka Fai Woo at the Department of Chemistry and Mr. Frank Ng at ITSC, for technical support. We gratefully acknowledge the financial support provided by the Research Grant Council, Hong Kong SAR Government, through the Project CUHK 4276/00P.

[1] A. C. Harms, S. N. Khanna, A. B. Chen, A. W. Castleman, Jr., *J. Chem. Phys.* **1994**, *100*, 3540.
[2] M. Sanekata, F. Misaizu, K. Fuke, S. Iwata, K. Hashimoto, *J. Am. Chem. Soc.* **1995**, *117*, 747.
[3] H. Watanabe, S. Iwata, K. Hashimoto, F. Misaizu, K. Fuke, *J. Am. Chem. Soc.* **1995**, *117*, 755.
[4] F. Misaizu, M. Sanekata, K. Fuke, S. Iwata, *J. Chem. Phys.* **1994**, *100*, 1161.
[5] F. Misaizu, M. Sanekata, K. Tsukamoto, K. Fuke, S. Iwata, *J. Phys. Chem.* **1992**, *96*, 8259.
[6] H. Watanabe, S. Iwata, *J. Chem. Phys.* **1998**, *108*, 10078.
[7] C. S. Yeh, K. F. Willey, D. L. Robbins, J. S. Pilgrim, M. A. Duncan, *Chem. Phys. Lett.* **1992**, *196*, 233.
[8] K. F. Willey, C. S. Yeh, D. L. Robbins, J. S. Pilgrim, M. A. Duncan, *J. Chem. Phys.* **1992**, *97*, 8886.
[9] P. E. Barran, N. R. Walker, A. J. Stace, *J. Chem. Phys.* **2000**, *112*, 6173.
[10] A. W. Castleman, Jr., K. H. Bowen, *J. Phys. Chem.* **1996**, *100*, 12911.
[11] A. W. Castleman, Jr., S. Wei, *Annu. Rev. Phys. Chem.* **1994**, *45*, 685.
[12] J. M. Lisy, *Int. Rev. Phys. Chem.* **1997**, *16*, 267.
[13] K. Fuke, K. Hashimoto, S. Iwata, *Adv. Chem. Phys.* **1999**, *110*, 431.
[14] G. Niedner-Schatteburg, V. E. Bondybey, *Chem. Rev.* **2000**, *100*, 4059.
[15] H. Watanabe, S. Iwata, *J. Phys. Chem. A* **1997**, *101*, 487.
[16] W. Y. Lu, S. H. Yang, *J. Phys. Chem. A* **1998**, *102*, 825.
[17] H. Watanabe, S. Iwata, *J. Phys. Chem.* **1996**, *100*, 3377.
[18] C. K. Siu, Z. F. Liu, J. S. Tse, *J. Am. Chem. Soc.*, submitted.
[19] M. Beyer, C. Berg, H. W. Gorlitzer, T. Schindler, U. Achatz, G. Albert, G. NiednerSchatteburg, V. E. Bondybey, *J. Am. Chem. Soc.* **1996**, *118*, 7386.
[20] M. Beyer, U. Achatz, C. Berg, S. Joos, G. Niedner-Schatteburg, V. E. Bondybey, *J. Phys. Chem. A* **1999**, *103*, 671.
[21] T. J. Selegue, J. M. Lisy, *J. Am. Chem. Soc.* **1994**, *116*, 4874.
[22] M. J. Frisch, G. W. Trucks, H. B. Schlegel, G. E. Scuseria, M. A. Robb, J. R. Cheeseman, V. G. Zakrzewski, J. A. Montgomery, Jr., R. E. Stratmann, J. C. Burant, S. Dapprich, J. M. Millam, A. D. Daniels, K. N. Kudin, M. C. Strain, O. Farkas, J. Tomasi, V. Barone, M. Cossi, R. Cammi, B. Mennucci, C. Pomelli, C. Adamo, S. Cliord, J. Ochterski, G. A. Petersson, P. Y. Ayala, Q. Cui, K. Morokuma, D. K. Malick, A. D. Rabuck, K. Raghavachari, J. B. Foresman, J. Cioslowski, J. V. Ortiz, A. G. Baboul, B. B. Stefanov, G. Liu, A. Liashenko, P. Piskorz, I. Komaromi, R. Gomperts, R. L. Martin, D. J. Fox, T. Keith, M. A. Al-Laham, C. Y. Peng, A. Nanayakkara, C. Gonzalez, M. Challacombe, P. M. W. Gill, B. Johnson, W. Chen, M. W. Wong, J. L. Andres, C. Gonzalez, M. Head-Gordon, E. S. Replogle, J. A. Pople, Gaussian 98, Gaussian, Inc., Pittsburgh, PA, **1998**.
[23] A. E. Reed, L. A. Curtiss, F. Weinhold, *Chem. Rev.* **1988**, *88*, 899.
[24] C. W. Bauschlicher, Jr., H. Partridge, *J. Phys. Chem.* **1991**, *95*, 9694.
[25] C. W. Bauschlicher, Jr., H. Partridge, *J. Phys. Chem.* **1991**, *95*, 3946.
[26] M. Sodupe, C. W. Bauschlicher, Jr., *Chem. Phys. Lett.* **1991**, *181*, 494.
[27] C. W. Bauschlicher, Jr., M. Sodupe, H. Partridge, *J. Chem. Phys.* **1992**, *96*, 4453.
[28] S. Sakai, *Bull. Chem. Soc. Jpn.* **1993**, *66*, 3326.
[29] J. Hrušák, D. Stöckigt, H. Schwarz, *Chem. Phys. Lett.* **1994**, *221*, 518.
[30] K. Hashimoto, K. Morokuma, *J. Am. Chem. Soc.* **1994**, *116*, 11436.
[31] K. Hashimoto, S. R. He, K. Morokuma, *Chem. Phys. Lett.* **1993**, *206*, 297.
[32] K. Hashimoto, K. Morokuma, *Chem. Phys. Lett.* **1994**, *223*, 423.
[33] K. Hashimoto, T. Kamimoto, *J. Am. Chem. Soc.* **1998**, *120*, 3560.
[34] K. Hashimoto, K. Morokuma, *J. Am. Chem. Soc.* **1995**, *117*, 4151.
[35] J. C. Thompson, *Electrons in Liquid Ammonia*, Oxford University Press, London, **1976**.
[36] Z. H. Deng, G. J. Martyna, M. L. Klein, *Phys. Rev. Lett.* **1993**, *71*, 267.
[37] T. Tsurusawa, S. Iwata, *J. Phys. Chem. A* **1999**, *103*, 6134.

Received: January 28, 2002 [F3826]

  0947-6539/02/0814-3186 $ 20.00+.50/0